Astron. Astrophys. 321, 189–201 (1997)

ASTRONOMY
AND
ASTROPHYSICS

Forbidden emission lines in Herbig Ae/Be stars⋆

M. Corcoran and T.P. Ray

School of Cosmic Physics, Dublin Institute for Advanced Studies, 5 Merrion Square, Dublin 2, Ireland

Received 16 July 1996 / Accepted 2 October 1996

Abstract. The absence of high velocity redshifted forbidden lines in classical T-Tauri stars (Appenzeller et al. 1984; Edwards et al. 1987) has long be taken as evidence of opaque circumstellar disks: disks which occlude the receding component of the stellar wind or outflow, allowing only the blueshifted emission to be observed. There has been some controversy in the literature recently as to whether a disk model is appropriate to the higher mass counterparts of the T-Tauri stars: the Herbig Ae/Be stars. With this controversy in mind, and a search for such occluding effects, we present part of a comprehensive study of 56 Herbig Ae/Be stars, 28 of which are observed to possess detectable [OI]λ6300 emission. It was found that those stars with [OI]λ6300 emission can be divided into four distinct groups as determined by line profiles and velocities. Roughly 15% (4) of the sample show both high and low velocity blueshifted forbidden emission lines reminiscent of the line profiles of classical T-Tauri stars with extended outflows. Of the three remaining groups, the first shows low velocity blueshifted emission with centroid velocities in the range -55 kms^{-1} $\leq$ v$_c$ $\leq$ -10 kms^{-1} (14 stars), the second unshifted ($|$v$_c|\leq$ 5 kms^{-1}) symmetrical forbidden emission lines (7 stars) and the third group of 3 stars low velocity (10 kms^{-1} $\leq$v$_c\leq$ 15 kms^{-1}) redshifted emission. No Herbig Ae/Be star was found to possess strongly redshifted forbidden line emission. The clear tendency towards blueshifted velocities not only implicitly suggests the presence of occluding disks around these stars but there also appears to be a link between the degree of embeddedness and the amount of forbidden line shift. An evolutionary effect may be responsible in the sense that, as the star becomes less enshrouded, the high velocity (jet) component of the forbidden line emission disappears first, followed by a decrease in the velocity of the low velocity component and finally by its disappearance altogether. The low velocity forbidden line emission is most likely a disk wind, the line profile being broadened as a result of the rotation of the disk. It is found that the line widths of the low velocity forbidden line emission are broader than those found in the classical T-Tauri stars. There is also evidence of acceleration in the outflow, traced by an increase in the blueshifted velocities from the [OI]λ6300 to the [SII]$\lambda\lambda$6717/6731 lines.

Key words: stars: mass-loss – stars: pre-main sequence – stars: circumstellar matter

1. Introduction

It has long been accepted that indirect evidence for circumstellar disks around low mass young stellar objects (YSOs) exists. Two of the primary arguments are observational: Firstly the inferred circumstellar masses of dust and gas surrounding classical T-Tauri Stars (cTTSs), measured by millimeter continuum observations, preclude a simple spherical distribution of the circumstellar material about such stars (Rydgren et al. 1982). The mass involved would, if spherically distributed, yield much higher optical extinctions than are actually observed (Lada & Adams 1992). Some alternate geometry, such as a disk, must exist to allow for both a substantial amount of circumstellar material and, at the same time, allow a relatively clear line of sight to the stellar surface. Secondly many cTTSs show blueshifted but not redshifted forbidden emission lines in their spectra, e.g. [OI]$\lambda\lambda$6300/6364, [NII]$\lambda\lambda$6548/6583, and [SII]$\lambda\lambda$6716/6731, indicative of low density gas envelopes or stellar winds. A large proportion of the observed [OI]λ6300 lines are highly blueshifted, with velocities in some cases of the order of -100 kms^{-1} (Edwards et al. 1987; Hartigan et al. 1995). One of the earliest explanations of the origin of these blueshifted profiles, from Appenzeller et al. (1983) and Appenzeller et al. (1984), invoked the presence of optically thick circumstellar disks which occlude the redshifted component of a stellar wind or other outflow close to the star. The subsequent success of disk models for cTTSs in explaining a variety of observational properties, such as the infrared excess and mass loss (see, for example, Edwards et al. 1993), supports the star+disk model as appropriate for low mass YSOs.

In the case of the more massive counterparts of the TTSs, the Herbig Ae/Be stars (HAEBESs), there remains considerable controversy in the literature about whether a significant fraction of these stars are surrounded by disks. For opposing views on this matter see Hillenbrand et al. (1992), Berrilli et al. (1992), Hartmann et al. (1993), Böhm & Catala (1994), Corcoran & Ray (1997a) and Ghandour et al. (1994). Certainly in a number of

Send offprint requests to: M. Corcoran

⋆ Based on observations made at the La Palma Observatory and the ESO/MPI 2.2m Telescope.

cases there is good evidence for disks: for example Grinin et al. (1994, 1996) and Grady et al. (1995) have observed polarimetric and photometric evidence, in a sample of HAEBESs, for an edge-on circumstellar disk-like envelope, associated with infall. It has been suggested that this subclass of HAEBESs, the UX Ori stars, may be the progenitors to stars similar to β Pictoris (Grinin et al. 1996). Here we take the approach that, as in the cTTSs, the forbidden lines can be used as a diagnostic for the presence of a disk.

Observations of forbidden lines, such as [OI]$\lambda\lambda$6300/6364 and [SII]$\lambda\lambda$6716/6731, however, in the case of the HAEBESS, are scarce. Finkenzeller (1985) published spectra of [OI]λ6300 forbidden line profiles of six HAEBESs and declared them to be "symmetrical to a good approximation." Nevertheless, deviations from symmetry were noted even by Finkenzeller (1985) in his small sample and, on close examination, all the profiles presented in Finkenzeller (1985) do show some degree of asymmetry. Böhm and Catala (1994) examined 33 HAEBESs for [OI]$\lambda\lambda$6300/6364 forbidden lines, using the interstellar absorption lines of neutral sodium (Na D) as an indirect measure of the systemic radial velocities of the stars. They found that roughly 50% (17) of the stars observed show the [OI]λ6300 line and only one of their sample (R Mon) shows strongly blueshifted emission in the fashion of young classical TTSs (Edwards et al. 1987, 1993). The "unshifted" lines of their sample show "symmetric profiles" with widths broadened to $\sim$ 30–100 kms^{-1}. R Mon, the only exception, is believed to possess a circumstellar disk (Koresko et al. 1993) and is known to be the source of both an optical and a molecular outflow (Mundt et al. 1987; Fukui et al. 1993).

Böhm & Catala (1994) have proposed that the "unshifted" forbidden [OI]λ6300 does not support the presence of circumstellar disks around their sample HAEBESs and may instead arise from a spherically symmetric wind or the sum of spherically distributed streams forming at the star. Given, however, the high wind velocities (several 100 kms^{-1}, Finkenzeller & Mundt 1984) inferred from the P-Cygni profiles of the permitted lines of these stars, it is somewhat difficult to see how such narrow forbidden line profiles (FWHM $\approx$ 30–100 kms^{-1}, Böhm & Catala 1994) could arise from a spherical wind.

In the case of the cTTSs, there is now considerable evidence that there are two distinct velocity components producing the forbidden emission lines (see, for example, Hamann 1994 and Hartigan et al. 1995). These components differ not only in velocity but in density as well (Hamann 1994). Moreover the high velocity component (hereafter the HVC) has been shown to be more spatially extended using high resolution long-slit spectroscopy (see, for example, Hirth et al. 1994a; Hirth 1994) than the low velocity component (or LVC). According to the model of Kwan and Tademaru (1988, 1995), the HVC and LVC are to be interpreted as the jet and disk wind respectively. To what extent is this picture relevant to the HAEBESs?

While a number of HAEBESs are known to possess clear LVC and HVC components in their forbidden emission lines (Hamann 1994; Böhm & Catala 1994), such stars are relatively rare. LkHα 233, PV Cep (Hamann 1994; Corcoran & Ray 1997b), V645 Cyg (Hamann & Persson 1989), and R Mon (Böhm & Catala 1994) all show blueshifted forbidden lines with typical velocities of a few hundred kms^{-1}. Moreover, in these cases, there is additional evidence that circumstellar disks exist for some of these stars, such as LkHα 233 and PV Cep which are both observed to have polarization patterns indicative of a disk-like geometry (Bastien & Ménard 1990; Gledhill et al. 1987). This paper presents the results of a survey of 56 Herbig Ae/Be stars, investigating their [OI]λ6300 forbidden emission lines (and in a few cases [SII]$\lambda\lambda$6717/6731 lines) and discusses the role of circumstellar disks as a possible means of explaining the results, with reference to the two-velocity outflow model of Kwan & Tademaru (1988, 1995).

2. Observations and data reduction

The observations of 56 HAEBES long slit spectra were obtained during three observing runs in La Palma on the Isaac Newton Telescope (INT) with the Intermediate Dispersion Spectrograph (IDS) in September 1991, July 1993 and December 1994. Further observations were kindly taken by Alan Moorhouse on La Silla with the ESO/MPI 2.2m Telescope using EFOSC-II in December 1991.

The La Palma data were taken at three different resolutions using the H1800V holographic grating and the R1200Y and R632V ruled gratings with GEC6 (Sept '91), EEV5 (July '93) and TEK3 CCDs (Dec '94) as detectors. The pixel size for all CCDs was 22μm. The corresponding dispersions for the three gratings were 0.22 Å/pixel for the H1800V grating, 0.36 Å/pixel for the R1200Y grating and 0.7 Å/pixel for the R632V grating, resulting in a velocity resolution (2 pixels) at Hα of 21 kms^{-1}, 34 kms^{-1} and 70 kms^{-1} respectively. The La Silla data was taken using a grism with a dispersion of 1.1 Å/pixel and a Thompson 1024 x 1024 CCD with a pixel size of 19μm and a velocity resolution of 105 kms^{-1}. Data reduction of the spectroscopy was carried out using standard IRAF[1] routines. Bias subtraction and flat-fielding corrections were determined from zero second exposures and tungsten lamp exposures respectively. The adjacent sky spectrum was subtracted from the object spectra, and the dispersion solutions were determined from CuAr arc exposures.

The velocity calibrations with respect to the stellar rest velocity are very important. Unfortunately in the wavelength range of the exposures encompassing the [OI]λ6300 lines, the coverage (e.g. 5850 – 6750Å with the R632V grating) does not include many photospheric lines that might serve to accurately determine the stellar rest velocity, V$_*$. Finkenzeller & Jankovics (1984) published radial velocities for 27 HAEBESs, measured from the shift of the narrow interstellar absorption lines of the Na D and CaII lines. They argued that both the interstellar lines of CaII and Na D have mean residual velocities close to those of the molecular clouds associated with the observed Herbig stars.

[1] The IRAF software is distributed by the National Optical Astronomy Observatories under contract with the National Science Foundation

Table 1. [OI]λ6300 line parameters and characteristic Hα profiles for the Herbig Ae/Be sample. W_λ is the [OI]λ6300 equivalent width, v_c the [OI]λ6300 centroid velocity relative to the estimated systemic velocity of the star, v_b and v_r the blue and red wing velocities respectively. Where there are two entries for v_c the star shows doubled-peaked emission at [OI]λ6300, and v_b is the blue wing of the high velocity component and v_r the red wing of the low velocity component respectively. The emission category is explained in the text. FWHM is corrected for the instrumental width. The profile of the Hα line is determined from our data, according to the criteria established by Finkenzeller & Mundt (1984). Those stars where the [OI] emission was unresolved in our spectra are listed as such. The average error in measuring v_c is $\pm$8 kms^{-1} except in those few stars observed at ESO which are marked with †, where the error is $\pm$18 kms^{-1}.

Name	W_λ (Å)	v_b (kms^{-1})	v_c (kms^{-1})	v_r (kms^{-1})	Emission Category	FWHM (kms^{-1})	Hα Profile
LkHα 198	1.37	-200	-20	+85	IIa	70	dbl.
V376 Cas	1.61	-125	-25	+50	IIa	100	P-Cyg.
BD+61° 164	0.18	-30	+10	+65	III	unres.	P-Cyg.
AB Aur	0.11	-30	0	+35	IV	unres.	P-Cyg.
HK Ori†	1.75	-240	-25	+110	IIa	100	sing.
HD 259431†	0.53	-150	-10	+135	IIb	100	sing.
R Mon	3.16	-210	-20	+240	IIa	110	dbl.
LkHα 25	1.63	-185	-15	+160	IIb	100	sing.
Z CMa†	0.93/1.61	-725	-450/-80	+160	I	205/320	P-Cyg.
NX Pup†	0.90	-270	-55	+185	IIa	90	sing.
Herbst 28†	0.17	-250	-10	+145	IIb	165	dbl.
HD 97048†	0.16	-170	-10	+100	IIb	100	P-Cyg.
KK Oph	1.61	-240	-35	+160	IIa	85	dbl.
ST 202	1.82	-165	-10	+115	IIb	70	dbl.
MWC 297	8.20	-30	+10	+55	III	unres.	sing.
VV Ser	0.44	-75	-5	+50	IV	50	dbl.
BD+40° 4124	1.10	-75	+5	+70	IV	50	dbl.
PV Cep	6.58/7.17	-455	-275/-60	+255	I	105/155	dbl.
AS 442	1.08	-200	-10	+80	IIb	195	dbl.
LkHα 134	0.50	-185	-10	+80	IIb	80	sing.
HD 200775	0.14	-40	+5	+80	IV	80	sing.
V645 Cyg	3.45/2.25	-550	-360/-55	+80	I	310/120	dbl.
LkHα 234	0.03	-95	+5	+90	IV	95	dbl.
BD+46° 3471	0.28	-85	+5	+40	IV	80	sing.
LkHα 257	0.10	-20	+15	+60	III	unres.	P-Cyg.
LkHα 233	0.52/0.50	-150	-115/-20	+70	I	80/150	P-Cyg.
MWC 1080	0.24	-155	-40	+75	IIa	90	P-Cyg.
LkHα 259	0.60	-45	+5	+65	IV	90	dbl.

Assuming that the majority of the line of sight absorption from Na D and CaII arises close to the HAEBESs in their associated clouds and that the young stars have velocities characteristic of their parent cloud velocity, the interstellar lines should have velocities that are approximately the same as those of the stars themselves. Finkenzeller & Jankovics (1984) found very good agreement between the measured velocities of Na D and CaII and the molecular cloud velocities measured by mm molecular line observations (see, for example, Edwards & Snell 1983) and quoted a mean residual velocity of -3.1 $\pm$ 3 kms^{-1} for the interstellar Na D absorption lines with respect to the associated molecular clouds. We have therefore used the interstellar absorption lines of Na D to determine the radial velocities of the stars in our sample.

In a number of cases it is possible to compare the radial velocity shift measured from the Na D with photospheric lines of iron, FeIλ6495 & FeIIλ6456, and from SiII$\lambda\lambda$6347/6371. The lines of silicon are at least partly chromospheric and as such may not truly represent the photospheric radial velocity. However, where the SiII lines are symmetric, the velocity shift agrees with that measured from the Na D lines and the FeI & FeII lines. The overall errors in the velocity measurements are between $\pm$5 kms^{-1} and $\pm$20 kms^{-1}, depending on the resolution of the grating. An average of $\pm$8 kms^{-1} is adopted for the INT data and an average of $\pm$18 kms^{-1} is adopted for the ESO data (as identified in Table 1).

It must be noted that for the purposes of velocity calibration, we have only used the narrow symmetric absorption lines of Na D , to insure that we measure the cloud gas velocities. Broader redshifted absorption lines in Na D , as observed, for example, by Graham (1992) and Grinin et al. (1994) have been modeled by Sorelli et al. (1996) as due to either magnetospheric accretion or the evaporation of star-grazing planetesimals.

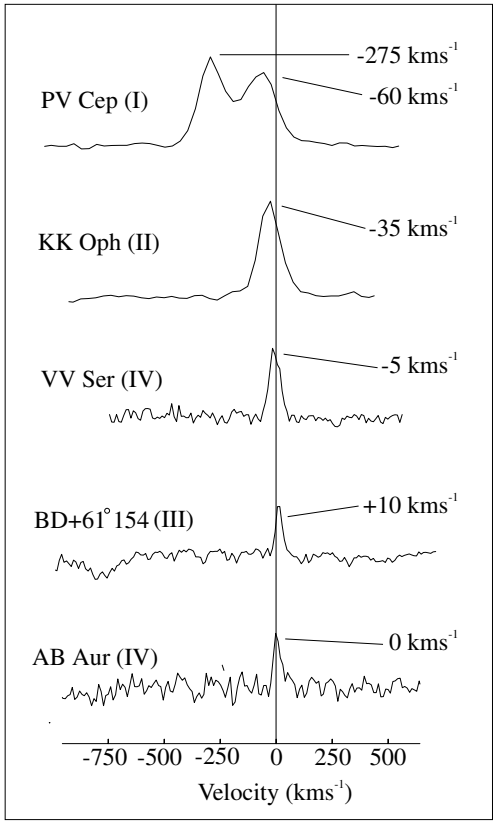

Fig. 1. [OI]λ6300 profiles of a selection of HAEBESs demonstrating the various categories defined in the text. The centroid velocities are marked. PV Cep clearly shows two emission components, one at high velocity and the other at a lower velocity. PV Cep is category I, KK Oph is category II, BD+61° 164 is category III, and VV Ser and AB Aur are in category IV. Note that on average the LVC emission in category I stars is more blueshifted than the LVC emission in the category II stars. See text for definition of the various categories.

3. Results

3.1. Low velocity forbidden line emission

From a sample of 56 Herbig Ae/Be stars we found 28 stars showing [OI]λ6300 emission. This detection rate of $\sim$ 50% is similar to that of Böhm & Catala (1994). The equivalent widths and velocities of the [OI]λ6300 lines are presented in Table 1. These 28 stars can be separated into different categories determined by the measured velocities and the profile of the line: I) High velocity ($|v_c| \geq$100 kms^{-1}) blueshifted emission, which may be accompanied by a low velocity blueshifted peak, II) low velocity (10 $\leq|$ $v_c|$ $\lesssim$55 kms^{-1}) broad (FWHM $\gtrsim$ 80 kms^{-1}) blueshifted emission, III) low velocity (10 kms^{-1} $\leq|v_c|\leq$15 kms^{-1}) redshifted emission with narrow lines, and IV) unshifted ($|v_c|\leq$5 kms^{-1}) emission with narrow lines. Each star is identified by this type in Table 1 and an example of each type of forbidden emission line is presented in Fig. 1. A histogram showing the distribution of [OI] centroid velocities is presented in Fig. 2.

In the first category there are four stars, V645 Cyg, Z CMa, PV Cep and LkHα 233, that show high velocity blueshifted emission. Centroid velocities for the HVC range from about -100 kms^{-1} to as high as -450 kms^{-1} in Z CMa. Velocities in the blue wing of Z CMa reach at least -700 kms^{-1}. All four stars also show double-peaked or P-Cygni profiles in their Hα lines, an indication of a stellar wind. These four stars are also known to be associated with stellar jets and/or molecular outflows: V645 Cyg is associated with a bipolar molecular outflow (Schulz et al. 1989; Verdes-Montenegro et al. 1991) and there are at least two Herbig Haro (HH) objects in its vicinity (Goodrich 1986; Hamann & Persson 1989). Z CMa drives a stellar jet (Poetzel et al. 1989) and a molecular outflow (Evans et al. 1994). It is also believed to be a FU Orionis object with a massive and highly active circumstellar disk (Malbet et al. 1993; Barth et al. 1994) and is therefore not likely to be a true HAEBES. Rather the object's high luminosity is due to its extremely high accretion rate. PV Cep is associated with a bipolar molecular outflow (Fukui et al. 1993) and HH emission (HH 215, Neckel et al. 1987) and LkHα 233 although not associated with a bipolar molecular outflow (Cantó et al. 1984; Leverault 1988) does illuminate a bipolar nebula (Staude & Elsässer 1993) and has a spectroscopically observed jet (Corcoran & Ray 1997b). All of these stars show two distinct velocity components at [OI]λ6300, with the LVC showing blueshifted velocities of less than 100 kms^{-1}. The LVC velocities are, however, higher on average than those of the LVCs observed in HAEBESs of category II.

In category II there are 14 stars, all showing low velocity blueshifted [OI]λ6300 emission, with velocities between -55 and -10 kms^{-1}. The stars in this category can be further subdivided into two groups of comparable size; those with intermediate blueshifted velocities, ranging from -55 kms^{-1} – -20 kms^{-1} (IIa), and those with low blueshifted velocities, ranging from -15 – -10 kms^{-1} (IIb). Of the 7 stars in category IIa, 5 are known to have associated molecular outflows and/or jets: LkHα 198 is associated with a highly collimated optical jet (Corcoran et al. 1995) and molecular outflow (Leverault 1988, Nakano & Tatematsu 1990). R Mon possesses a stellar jet (Mundt et al. 1987) and a molecular outflow (Cantó et al. 1981) as has MWC 1080 (Poetzel et al. 1992; Yoshida et al. 1992). V376 Cas has both HH objects in its vicinity and possibly a molecular outflow (Corcoran et al. 1995; Leinert et al. 1991; Piirola et al. 1992) while HK Ori may be associated with HH objects (Goodrich 1992). Only NX Pup and KK Oph have no observations of such outflow phenomena in the literature. In category IIb there are 7 stars, none of which is associated with a molecular outflow in the lists of Fukui et al. (1993) or a bipolar nebula in Staude & Elsässer (1993). No optical jets or HH objects are mentioned in the literature in connection with any of these 7 stars.

It seems plausible that the stars in category IIa are similar to those in category I, except for the "absence" of the HVC in the [OI]λ6300 emission. This "absence" may not be real in some cases but instead may be due to the orientation of the outflow. Another possible cause is an intermittancy effect (see below). Those stars in category IIb are, for the most part, lacking any evidence for extended outflows. Of course the effect of inclination will play an important part in determining the radial velocity of any [OI]λ6300 line. Some of the stars in category IIa

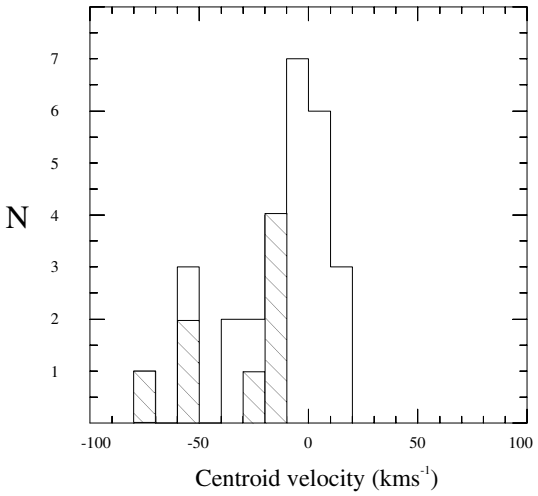

Fig. 2. A histogram plot of the centroid velocities of the LVC [OI]λ6300 line from the sample. The binwidth is 10 kms^{-1}. Note that the majority of stars show velocities in the range -40 kms^{-1} to +10 kms^{-1}. The cross-hatched stars are those in Hillenbrand's (1992) Group II and are thought to be the relatively least evolved HAEBESs; they occupy the left of the distribution. The remainder are all Hillenbrand (1992) Group I stars. There is no corresponding group of stars with even moderately redshifted forbidden line emission.

are believed to have outflows in the plane of the sky, for example, LkHα 198 and R Mon (Corcoran et al. 1995; Brugel et al. 1984). As a result the HVC and LVC emission may be unresolved. The spatial orientation of the outflow from V376 Cas is unknown, but it is plausible to assume that, like its neighbour LkHα 198, its outflow axis is also in the plane of the sky, given the tendency for outflows in the same area to be aligned (Reipurth 1989).

Category III has only three stars, BD+61° 164, MWC 297 and LkHα 257, all of which showed redshifted [OI]λ6300 emission at low velocities (+10 $\lesssim$ v$_c$ $\lesssim$ +15 kms^{-1}). None of these stars are known to be associated with jet or molecular outflow activity. Finally, category IV has seven stars all showing small shifts in [OI]λ6300 velocities within the range -5 kms^{-1} $\leq$ v$_c$ $\leq$ 5 kms^{-1}. Due to the limitation of the errors in the centroid velocities it may be that categories III and IV are not distinct groups. If this is the case there may be no HAEBESs with genuinely redshifted [OI]λ6300 emission in our sample.

Clearly there is not a symmetrical distribution of [OI]λ6300 velocities about 0 kms^{-1} in the histogram (Fig. 2). In *contrast* to the histogram published in Böhm & Catala (1994) the distribution indicates *that most HAEBESs show low velocity blueshifted forbidden line emission*.

As well as observations of the [OI]λ6300 line, our spectra also include the [SII]$\lambda\lambda$6716/6731 forbidden line doublet. These lines have a critical density roughly 150 times lower than the [OI] doublet (Osterbrock 1989) and can be used to probe low density regions. None of the stars observed in the sample that do not show [OI]λ6300 emission display [SII]$\lambda\lambda$6716/6731 emission. Of the 28 stars that do show [OI]λ6300, 9 display detectable levels of [SII]$\lambda\lambda$6716/6731 (see Table 2). One star, ST 202, is left out of Table 2 due to lack of information about its distance and absolute flux levels. It is interesting to note that 7 of these 9 stars with [SII]$\lambda\lambda$6716/6731 emission also have definite associations with molecular outflows and/or HH jets and objects. For the other 2 stars (KK Oph and ST 202) with [SII]$\lambda\lambda$6716/6731 emission, observations are lacking that would confirm or refute the hypothesis that all HAEBESs with [SII]$\lambda\lambda$6716/6731 emission possess extended outflows. In any event all of the stars, except ST 202, with detectable [SII] emission either fall into our category I or category IIa.

It is relatively straightforward to derive a value for the mass loss rate for a wind from a young stars based on the luminosity of forbidden lines. As such lines are optically thin, their luminosities are proportional to the total number of radiating atoms along the line of sight and consequently proportional to the total mass in the radiative component of the flow. The mass loss rate $\dot{M}_{wind}$ is found from the mass of the high velocity component, the flow speed and a scale length, l of the emission, where $\dot{M}_{wind} = MV/l$ (see for example Hartigan et al. 1995). Using the luminosity of the [SII]λ6731 line we have estimated the mass loss rates of 9 HAEBESs. This line comes from the ^{2}D$_{3/2}$ to ^{4}S$_{3/2}$ transition of singly ionized sulphur. Assume the total luminosity of the [SII]λ6731 line is L$_{21}$, then

$$L_{21} = \eta_2 A_{21} h\nu_{21} \quad (1)$$

$$= \frac{g_2}{g_1}\eta_1 \exp\frac{-h\nu_{21}}{kT}(1+\frac{N_{crit}}{N_e})^{-1} A_{21} h\nu_{21} \quad (2)$$

where η_1, η_2 are the number of S$^+$ ions in the emitting region in the lower and upper states, 1 and 2, respectively; A$_{21}$ is the Einstein coefficient for the λ6731 transition and is 8.82 $\times$ 10^{-4} s^{-1} (Mendoza 1983); hν_{21} is the energy of the transition and is 2.95 $\times$ 10^{-12} ergs; g$_1$, g$_2$ are the statistical weights of the two levels and are 10 and 4 respectively; T is the temperature at which the transition takes place, N$_e$ is the electron density; and N$_{crit}$, the critical density for the transition, is equal to $\frac{A_{21}}{C_{21}}$ where C_{21} is the collisional de-excitation rate. The exact temperature for the transition is uncertain and can be estimated from ratios of forbidden lines with well separated energies. Unfortunately we lack observations of the appropriate lines to allow derivations of electron temperatures. The calculations of Kwan and Tademaru (1995) indicate electron temperatures in the range 3000 K to 10^4 K and above. For the purposes of the calculation here a representative value for the electron temperature of 10^4 K is used; an electron temperature of 5 $\times$ 10^3 K produces a resultant mass loss rates on average a factor of 2 higher. Table 2 presents the calculated mass loss rates.

C$_{21}$, the collisional de-excitation rate is given by

$$C_{21} = \frac{8.63\times10^{-6}\Omega_{21}}{g_2 T(K)^{1/2}}\mathrm{cm^3 s^{-1}} \quad (3)$$

where Ω_{21} is the collision strength. The collision strength of the [SII]λ6731 line is $\Omega_{21} \sim 2.79$ (Mendoza 1983). The critical density is 1.47 $\times$ 10^4 cm^{-3} for T = 10^4 K, and 1.04 $\times$ 10^4 cm^{-3} for T = 5 $\times$ 10^3 K.

Table 2. Mass loss rates calculated from the luminosity of the [SII]λ6731 line in 8 Herbig Ae/Be stars. See Sect. 3.1 for a discussion of the calculation of the mass loss rate for the HVC and LVC. The first four stars have clearly separated HVC and LVC emission, although this is not the case for the last four stars. Here v_c is the radial velocity of the profile centroid. Note that v_c is larger for the [SII] line than the [OI] line for all stars except Z CMa. The values for $V_\perp$ are estimated tangential velocities. The mass loss rate are calculated for an electron temperature of 10^4 K and show an average increase of a factor of 2 for an electron temperature of 5×10^3 K. The HVC velocities marked with a † are representative values assumed for the HVC. It is not clear in these cases whether we are observing a HVC, LVC or, possibly, a combination of both. The entries in the last column therefore should be seen as indicative of the mass loss range. The HVC velocity of R Mon, marked *, is taken from the tangential jet velocity of the associated jet (Mundt et al. 1987).

Name	L_{6731} ($10^{-4}L_\odot$) HVC/LVC	N_e (cm^{-3}) HVC/LVC	D (pc)	v_c(kms^{-1}) HVC/LVC	$V_\perp$(kms^{-1}) HVC/LVC	$\dot{M}_{wind}$ ($M_\odot yr^{-1}$) HVC/LVC
Z CMa	1380/957	500/1000	1150	-325/-60	560/105	1.2×10^{-4}/2.5×10^{-5}
PV Cep	6.29/6.69	3300/14000	500	-300/-75	520/130	2.2×10^{-7}/6.3×10^{-8}
V645 Cyg	157/39.5	10000/8000	3500	-375/-70	650/125	4.4×10^{-7}/7.3×10^{-8}
LkHα 233	9.64/12.2	650/2000	880	-125/-25	215/45	3.4×10^{-7}/9.5×10^{-8}
LkHα 198	2.69	3000	600	–/-35	300†/60	4.8×10^{-8}/2.9×10^{-8}
V376 Cas	2.04	1500	600	–/-30	300†/50	6.9×10^{-8}/3.3×10^{-8}
R Mon	76.6	6000	800	–/-25	300*/45	6.0×10^{-7}/2.7×10^{-7}
KK Oph	0.83	14000	160	–/-25	300†/45	1.9×10^{-8}/8.7×10^{-9}

To make an estimate of the total luminosity from the [SII]λ6731 line it is necessary to determine the number of S^+ ions in the emitting region. This is done as follows: The total number of S^+ ions at level 1 in the emitting region or aperture, η_1, is

$$\eta_1 = (\frac{\eta_1}{\eta(S^+)})(\frac{\eta(S^+)}{\eta(H)})(\frac{\eta(H)}{\eta_{total}})(\frac{M_{total}}{\mu m_H}) \quad (4)$$

where $\eta(S^+)$ is the number of S^+ ions in the emitting region; η(H) is the number of hydrogen atoms in the aperture; η_{total} is the total number of atoms of all species in the aperture; and M_{total} is the total mass in the aperture. For solar abundances (Allen 1973) the mean molecular weight, μ, for a neutral atomic gas is 1.24, $\eta(S^+)/\eta$(H) is 1.86×10^{-5}, assuming all the sulphur is ionised, and η(H)/η_{total} is 0.921. We assume that $\eta_1/\eta(S^+) \approx 1$ for $T \geq 10^4$ K. Combining these values gives a value of $\eta_1 = 4.14 \times 10^{-15}\ M_{total}$ for M_{total} in units of $M_\odot$. Substituting this value of η_1 into the earlier equation (eqn. 2) for L_{21} (i.e. L_{6731}):

$$M_{total} = 4.3 \times 10^{-4}(1 + \frac{N_{crit}}{N_e})(\frac{L_{6731}}{L_\odot})M_\odot \quad (5)$$

for the mass within the emitting region for an electron temperature of 10^4 K. A similar calculation can be carried out for an electron temperature of 5×10^3 K.

To calculate the mass loss rate we take a length scale, $l_\perp$, the projected aperture size on the sky, and a velocity, $V_\perp$, the projected velocity on the sky. The mass loss rate is then $\dot{M} = MV_\perp/l_\perp$. Finally then the mass loss rate as determined from the luminosity of the [SII]λ6731 line is

$$\dot{M}_{wind} = 9.1 \times 10^{-3}(1 + \frac{N_{crit}}{N_e})(\frac{L_{6731}}{L_\odot}) \quad (6)$$

$$\times (\frac{V_\perp}{100 kms^{-1}})(\frac{l_\perp}{pc})^{-1} M_\odot yr^{-1} \quad (7)$$

where $V_\perp$ is the jet velocity in the plane of the sky and $l_\perp$ is the size of the aperture. For $V_\perp$ we assume an average orientation angle of the various outflows relative to the line of sight of $\sim 60°$ and calculate $V_\perp$ from the measured radial velocities (Table 2), except in the case of R Mon, where independent observations suggest that the outflow is practically in the plane of the sky (Mundt et al. 1987). The tangential velocity cited by Mundt et al. (1987) for the R Mon jet (HH 39) is $\sim$ 300 kms^{-1} while the heliocentric radial velocity they cite is -75 kms^{-1}. In fact the radial velocity is actually that of the bipolar jet close to the star (4"–10", Brugel et al. 1984) and the tangential velocity that of HH 39, much further away. If we assume that the outflow undergoes no significant change in velocity between the two regions, the inferred orientation angle is $\sim 15°$. The value of $l_\perp$ for the HVC is the average slit width or $\sim$ 1.5". For the LVC this is clearly an overestimate of the size of the emitting region. Observations of LVC emission in TTSs by Solf & Böhm (1993) and Hirth (1994) suggest that the LVC extends a distance of $\sim$ 0.1 – 0.2" from the star. In our observations (Corcoran & Ray 1997b) we find that the LVC emission from the HAEBES PV Cep, for example, extends approximately 0.5" from the star. Consequently we choose an approximate value of 0.5" for $l_\perp$ here.

The approximate estimates of mass loss rates, $\dot{M}_{wind}$, for the 8 stars with detected [SII] emission are listed in Table 2 (ST 202 is left out due to insufficient data about distance and absolute flux). For the 4 stars (Z CMa, PV Cep, V645 Cyg and LkHα 233) with distinct HVC and LVC emission, corresponding separate values of $\dot{M}_{wind}$ are listed. In the case of the other 4 stars the [SII] lines cannot be separated into clear HVC and/or LVC emission. Consequently the mass loss rates in Table 2 for these stars (LkHα 198, V376 Cas, R Mon and KK Oph) are calculated for two distinct cases: Pure HVC emission and pure LVC emission. Without resolving the two components no more definite values can be given.

Table 3. Measurements of the equivalent width of the [OI]λ6300 line in Herbig Ae/Be stars observed by Finkenzeller (1985), Böhm & Catala (1994) and ourselves. The date of observation is given in parentheses (day.month.year). Errors are $\pm$5% – $\pm$10%, depending on the individual observations. The absolute visual band variability, $\mid \Delta M_v \mid$, where known, is taken from Finkenzeller & Mundt (1984).

Name	$\mid \Delta m_v \mid$	W_λ(Å) (this work)	W_λ(Å) (Finkenzeller)	W_λ(Å) (Böhm & Catala)
BD+61° 154	0.37	0.18 (3.9.1991)	–	0.23 (24.10.1991)
AB Aur	0.15	0.11 (3.9.1991)	–	0.125 (16.12.1991)
HK Ori	0.20	1.75 (23.12.1991)	1.8 (18.11.1981)	–
HD 259431	0.01	0.53 (26.12.1991)	0.5 (16.11.1981)	0.50 (22.10.1991)
R Mon	0.87	3.16 (1.1.1992)	–	1.2 (30.1.1986)
NX Pup	0.05	0.90 (25.12.1991)	–	0.83 (30.01.1991)
HD 97048	0.07	0.16 (1.1.1992)	–	0.19 (29.1.1986)
KK Oph	0.6	1.61 (5.6.1991)	1.4 (21.5.1981)	–
HD 200775	0.05	0.10 (1.9.1991)	–	0.12 (22.10.1991)
BD+40° 4124	0.07	1.10 (1.9.1991)	1.5 (16.6.1981)	–
BD+46° 3471	0.07	0.28 (1.9.1991)	–	0.10 (22.10.1991)
LkHα 218	–	$\leq$0.04 (25.12.1991)	–	0.19 (30.1.1986)
LkHα 220	–	$\leq$0.1 (25.12.1991)	–	0.29 (30.1.1986)
MWC 137	–	$\leq$0.15 (31.12.1991)	0.8 (16.11.1981)	–

The mass-loss rates are typically 10–100 times higher than those observed for cTTSs (Hartigan et al. 1995). We emphasize that the mass loss rates are order of magnitude estimates only, as they are strongly dependent on the temperature.

Other methods of estimating the mass loss rate exist and give varying values, examples include Hollenbach (1985) where the mass loss rate is derived from the luminosity of the [OI]63μm line assuming each atom passes through only one shock and Poetzel et al. (1992) where $\dot{M}$ is derived from the visible jet parameters. See Hartigan et al. (1995) and Kwan & Tademaru (1995) for a discussion. Nisini et al. (1995) make direct estimates of the mass loss rate from the luminosities of infrared lines of neutral hydrogen. In this case there is a possibility that there is a contribution from infalling material (G. Gahm, private communication) as in the model of Sorelli et al. (1996) which would strongly affect the derived mass loss rates.

3.2. Emission line variability

The observations presented here, in conjunction with other published data (Finkenzeller 1985; Böhm & Catala 1994) provide a useful database for some comments on line variability in the [OI]λ6300 line. For those stars observed by Finkenzeller (1985), comparisons of velocities and equivalent widths are possible over a time scale of roughly ten years. Of the six stars presented in Finkenzeller (1985) showing [OI]λ6300 emission we have spectra of 5 stars; KK Oph, BD+40° 4124, HD 259431, MWC 137, and HK Ori. Of the 13 stars observed by Böhm & Catala (1994), not taken from the sample of Finkenzeller (1985), we have spectra of 10 stars; BD+61° 164, AB Aur, HD 259431, LkHα 218, LkHα 220, NX Pup, HD 97048 HD 200775, BD+46° 3471 and R Mon. The variations in observed equivalent widths of all 14 stars (HD 259431 being present in all three samples) are presented in Table 3. Note that variation in the equivalent width may arise from changes in the continuum level and the variability discussed here may reflect this. However in those cases where a variation in velocity is also observed it is obvious that properties of the line emitting region are varying in addition to any contribution from variations in the stellar continuum level.

Of the 14 stars, 9 show little or no variation ($\leq$ 0.2Å) in the equivalent width of the [OI]λ6300 line over timescales up to 10 years. The remaining five stars, LkHα 218, LkHα 220, BD+40° 4124, R Mon and MWC 137, show variations ranging from a 30% reduction in W_λ([OI]) over 10 years for BD+40° 4124 to as much nearly a 300% increase in the line equivalent width in R Mon over six years. Given the length scales and velocities involved, it is possible to imagine a situation where the outflow characteristics vary with timescales of order 5–10 years, so perhaps the observed variations are not surprising. Note that although the sample presented here only contains one Hillenbrand Group II star (R Mon), this star shows the greatest variation in the observed equivalent width.

Of the 14 stars observed in common with Finkenzeller (1985) and Böhm & Catala (1994), published centroid velocities are available only for the data of Böhm & Catala (1994). Three stars show different centroid velocities in our observations to the observations of Böhm & Catala (1994). HD 259431 and NX Pup (CoD -42° 3318) have changed by -20 kms^{-1} and -40 kms^{-1} respectively. HD 259431 shows a change from +7 kms^{-1} on 22.10.1991 to -10 kms^{-1} on 26.12.1991 and NX Pup shows a change from -15 kms^{-1} in 30.01.1986 to -55 kms^{-1} in 25.12.1991. Neither of these stars is observed to vary strongly in the equivalent width of the [OI]λ6300 line. The only star showing a dramatic change in both the line profile and velocity is R Mon. From a strongly asymmetric and blueshifted line with a centroid velocity of -35 kms^{-1} and a bluewing velocity of -140 kms^{-1} on 30.01.1986 (Böhm & Catala, 1994) the profile had changed to a fairly symmetrical profile shifted to only -20 kms^{-1} on 1.1.1991. As only R Mon shows variation both in the equivalent width and the centroid velocity of the [OI]λ6300 line it is not clear whether the variability in the line width in the other stars here is due to continuum variability or an actual change in the line forming region.

Table 4. Spectral type identifications from comparisons with standard stars over the spectral ranges 4200 – 5100Å and 5850 – 6750Å, and from Thé et al. (1993) and Finkenzeller & Mundt (1984).

Name	Spectral Type (obs.)	Spectral Type (Thé/F+M)
NX Pup	A7-A9	A-Fe/A1
LkHα 215	B8-B9	B7-B8e/B5
V1686 Cyg	A0	B2-B3e/B5
LkHα 234	B6-B7	B5-B7e/B3
LkHα 134	B9-A1	B8-Ae/B2

3.3. Spectral type identification

Using standard star spectra taken simultaneously with the INT data from July 1993 we are able to make comparisons of the spectral types of a number of HAEBESs in our sample with those spectral types quoted in the literature (Finkenzeller & Mundt 1984; Thé et al. 1993). Of the stars examined (56), 5 stars show absorption features indicative of a distinctly different spectral type (more than 3 subclasses) to some values quoted in the literature. The spectral type of the stars was determined from the lines of HeIλ4471, MgIIλ4481 (Lang 1991). It must be noted that a number of stars (e.g. V645 Cyg, MWC 1080) show P-Cygni profiles in many of the blue lines often used in determining a star's spectral type and more generally, levels of photospheric veiling such that we are unable to confirm the accuracy of the spectral type identifications for such stars usually quoted in the literature. The results of this investigation, and the spectral types cited in the literature are presented in Table 4.

4. Discussion

4.1. Forbidden line emission

Kwan & Tademaru (1988) proposed that the double-peaked profile observed in the [OI]λ6300 lines of many TTSs is in fact due to two separate outflow processes, each with distinct velocities. Their model invokes for the fast component an initially radially expanding wind which is collimated by the magnetic field of the circumstellar disk. For the slow component, they propose a wind from the circumstellar disk and/or a warm disk corona. Such a model naturally predicts the double-peaked structure observed, for example, by Edwards et al. (1987). Kwan & Tademaru (1995) have recently developed a model of a rotating disk wind to explain the origin of the LVC emission in cTTSs, caused by a magnetic torque and centrifugal flinging. The mass loss rate for such a disk wind is considerably smaller ($\leq$ 10%) than that of the jet responsible for the HVC emission.

To what degree is this model applicable to HAEBESs? Before examining this idea we should consider what our observations tell us about the possibility of disks around HAEBESs. As described in the Results section, the [OI]λ6300 forbidden line emission falls into one of four categories, examples of which are shown in Fig. 1. Of those stars in emission category I, all are known to drive either stellar jets and/or molecular outflows (see, for example, Mundt & Ray 1994, Fukui et al. 1993). The relative scarcity of HVC forbidden emission lines in HAEBESs may be taken, in terms of the Kwan and Tademaru (1988) model, as indication that the number of HH jets amongst this class is small. This is born out by imaging studies (e.g. Mundt & Ray 1994). Moreover Bastien & Ménard (1990) have observed the polarization patterns, in both the optical and infrared, of a number of HAEBESs and we note that three of the category I stars (V645 Cyg, LkHα 233 and PV Cep) and one of the category II stars (R Mon) all show polarization patterns indicative of multiple scattering from a flattened disk-like structure.

In category II we find the largest single group of the observed stars, with 14/28 stars (50%) showing low (-10 kms^{-1} – -55 kms^{-1}) velocity blueshifted lines. There is essentially no corresponding redshifted group; the majority of the remaining [OI]λ6300 profiles clustering closely around zero velocity. Only BD+61° 164 shows a redshifted velocity over +10 kms^{-1}. All the category II stars that have detected [SII]$\lambda\lambda$6716/6731 emission (the 4 category II stars in Table 2 plus ST 202) have other indications of mass loss and extended outflows, apart from ST 202 which has not been included in any published molecular or optical outflow study. In contrast none of the category II stars without [SII]$\lambda\lambda$6716/6731 emission show any indications of jets or outflows, except MWC 1080 which has weak [SII] emission detected by Poetzel et al. (1992). It is therefore interesting to note that in the case of cTTSs, those stars with low veiling continua, and consequently low inferred accretion rates, show unshifted and symmetric profiles of [OI]λ6300 and weak or absent [SII]$\lambda\lambda$6716/6731 emission (Edwards et al. 1987; Hartigan et al. 1995) .

Knowing that essentially all the category I stars and many of the category IIa stars are outflow sources and also show [SII]$\lambda\lambda$6716/6731 emission, it is tempting to suggest that the presence of [SII]$\lambda\lambda$6716/6731 indicates a certain degree of outflow activity that the stars without [SII]$\lambda\lambda$6716/6731 emission lack. Whether this is simply a matter of the relatively higher rates of accretion producing relatively higher mass loss rates and consequently brighter forbidden lines (Corcoran & Ray 1997a) or because the origin of the observed [SII] emission (and more generally, all forbidden line emission) differs between the stars with outflows and the other categories (IIb, III and IV) is not clear.

The mechanism that gives rise to the forbidden LVC emission appears much the same in both category I and II, with respect to the line widths and profiles, although as noted the LVC blueshifted velocities are uniformly higher in the category I sources. It may be that the mechanism for accelerating the HVC material entrains LVC material and accelerates it to the higher velocities seen, as described in the models of Königl (1989, 1991) and Safier (1993a,b).

The centroid velocity of the [OI]λ6300 emission in our few category III stars is only marginally redshifted (+10 kms^{-1} $\leq$ v$_c$ $\leq$ 15 kms^{-1}). The simplest explanation is that these small redshifts are due to deviations from the zero velocity caused by the method used; e.g. velocity differences between the stellar velocity and the bulk gas velocity responsible for the Na D absorption lines. No molecular or optical outflow is associated with any of the category III stars. The 7 stars in category

IV have symmetric and unshifted profiles, centred on the stellar rest velocity. In this regard it is interesting to note that LkHα 234 (Ray et al. 1990) and BD+46° 3471 (Goodrich 1992) are both in category IV and have been regarded as possible sources of a jet and a HH object respectively. However, a close-by embedded infrared companion to LkHα 234, recently discovered by Weintraub et al. (1994) now appears to be the true source of the jet. Whether an infrared companion can also explain the case of BD+46° 3471 is worth investigating. None of the other category IV stars is associated with a molecular or optical outflow. Moreover, none of the category III or IV stars show [SII]$\lambda\lambda$6716/6731 emission.

It was mentioned in Sect. 3.1 that our results conflict with those of Böhm & Catala (1994), and in particular the clear preference we find for the centroid velocity of the LVC to be blueshifted argues strongly against the spherical wind model of Böhm & Catala (1994). At best this model can only apply to a small subset of the HAEBESs. It must be noted that our sample contains many more Hillenbrand Group II stars (Hillenbrand et al. 1992), which are those HAEBESs that show flat or rising spectra in their spectral energy distributions, than the sample of Böhm & Catala (1994). This may in part influence the distribution of [OI]λ6300 emission, as the Group II stars are believed to be less evolved and potentially more active in terms of outflows (Hillenbrand et al. 1992). Certainly all the stars in our sample that show high velocity blueshifted emission (category I) are Hillenbrand Group II stars. In the sample presented here 10 out of 28 stars are the sources of molecular outflows, jets and/or HH objects. Böhm & Catala have only 3 such sources out of 17 stars. Moreover none of the stars observed by Böhm & Catala with the MUSICOS echelle spectrograph show any [SII]$\lambda\lambda$6716/6731 emission. As already mentioned, emission from [SII]$\lambda\lambda$6716/6731 appears to be connected to the conditions that give rise to jets.

Although the centroid velocities of the LVC are blueshifted in most cases, it is nevertheless very interesting that the LVC is very broad with significant blue and red wings, at least for the category I and II stars. If, as we do here, one attributes the LVC to a disk wind along the lines of the model of Kwan & Tademaru (1988, 1995) then the broadness of the component cannot be understood in terms of a poorly collimated wind but instead may be due to the rotation of the disk (see below).

A number of important results stem from the observation of low velocity blueshifted components in the forbidden lines of HAEBESs. Firstly, the systematic blueshift of the [OI]λ6300 line in a majority of cases parallels what is seen amongst the cTTSs. Moreover the analogy between the two groups is strengthened further with the discovery that the equivalent width of the [OI]λ6300 line scales with the near-infrared colour in the same way as the cTTSs (Corcoran & Ray 1997a). In cTTSs the consistent blueshifts of the forbidden lines are taken as evidence of the presence of optically thick circumstellar disks, which occlude the receding outflow, leaving only the blueshifted material visible to the observer. While in the case of the HAEBESs only $\sim$10% of the observed stars show strongly blueshifted lines similar to those observed in classical TTSs, a majority of the observed Herbig stars do show a low velocity blueshift. In Fig. 2 we displayed a histogram of the distribution of centroid velocities for the [OI]λ6300 LVCs in our sample. As the plot shows there is a distinct asymmetry to the distribution of the LVC centroid velocities, with no group of HAEBESs with moderately redshifted forbidden emission lines. Only 5 stars show centroid velocities blueshifted by -40 kms^{-1} or greater, 3 of which are the LVC components of double component (i.e. HVC plus LVC) profiles (V645 Cyg, Z CMa & PV Cep).

Thus, although the presence of disks around HAEBESs in all cases may still be in question, the observations presented here of a blueshifted asymmetry in both the HVCs and LVCs show that disks almost certainly exist around many HAEBESs. These disks could be purely reprocessing or actively accreting or a combination of both processes. The outflow sources have jets, forbidden lines, molecular outflows and other indicators of activity very similar to the cTTSs that also show the best evidence for circumstellar disks.

Turning now to the possibility of an evolutionary sequence amongst the surveyed stars, if, as might be suspected from their degree of embeddedness (Hillenbrand et al. 1992), the Hillenbrand Group II stars represent the relatively less evolved HAEBESs, it may be possible to construct an evolutionary sequence for the various HAEBESs using their degree of outflow activity. We place the category I stars, as the least evolved stars, at the beginning of the sequence. Consisting mainly of Hillenbrand Group II stars they are believed to be comprised of a central star surrounded by a disk plus a dusty envelope (Hillenbrand et al. 1992; Natta et al. 1993a,b). Of the 4 stars in category II with [SII]$\lambda\lambda$6716/6731 emission, 2 stars (R Mon & V376 Cas) also have indications of outflows and/or jets (Brugel et al. 1984; Corcoran et al. 1995). These stars we also place at the beginning of the evolutionary sequence.

Those category II stars that have no detectable levels of [SII]$\lambda\lambda$6716/6731 emission but do have blueshifted [OI]λ6300 emission at low velocities are probably representative of the more evolved state where the conditions for high velocity extended outflows have died away, be it from a weakening of a disk magnetic field that might be responsible for accelerating a jet or a reduction in the accretion rate that would have powered the high velocity outflow. The inner regions of the disk may still produce weak [OI]λ6300 emission in a disk wind or warm disk corona (see §4.2) as proposed by Kwan & Tademaru (1988) but any associated [SII]$\lambda\lambda$6716/6731 emission is too weak to be observed. Alternatively the category II stars may represent quiescent jet/outflow sources. The latter idea, however, seems less likely given the lack of known molecular outflows associated with these stars. Specifically, according to Padman & Richer (1994) molecular outflows have characteristic timescales that are much longer than the inferred dynamical timescales. The lifetimes of molecular outflows ($\sim 10^5$ yrs) are such that intermittancy in a stellar jet driving the outflow would not allow the molecular outflow to dissipate in the short time when the jet is in a quiescent state ($\leq 10^3$ yrs, the dynamical time scale for a typically observed jet, Mundt et al. 1990).

As the system evolves the disk may at some point have lost sufficient mass through the action of a stellar wind or other mass loss process to render it optically thin (see Strom et al. 1993 and Wolk & Walter 1996 for possible examples of TTSs with such disks). At such a stage both the redshifted and blueshifted parts of a stellar or disk wind should be visible and perhaps no longer collimated by the action of the disk or its magnetic field. The resulting profile produced by the combination of the two portions of the wind will be unshifted and symmetric, broadened to roughly twice the outflow velocity, if viewed edge-on. The category IV stars show just such emission and may be considered to be the most evolved of the [OI]λ6300 stars. Alternatively the category IV stars may have completely dispersed their circumstellar disks, and produce the [OI]λ6300 emission in the manner proposed by Böhm & Catala (1994) as a spherically symmetric wind or a sum of spherically symmetric distributed streams forming at the surface of the star which produce shocks at great distances from the star. Given however the apparent power law proportionality between infrared excess and the strength of the forbidden line emission (Corcoran & Ray 1997a) for all the [OI]λ6300 emitting HAEBE stars, we favour the idea that one mechanism is responsible for the outflow properties of all categories. Fig. 3 shows a possible evolutionary sequence from the category I to category II & IV stars.

The proposed evolutionary sequence involves the evolution of the stellar wind. Initially the wind, presumably driven by accretion, has a high velocity and may be collimated and drive an outflow, as is found in the partially embedded (Hillenbrand Group II) stars. Then as the star and circumstellar material evolve the wind velocity decreases, perhaps as the accretion rate drops, and the wind is characterized by the lower blueshifted velocities seen in the category II stars ([OI]λ6300 centroid velocities of $\leq$ -50 kms^{-1}). In the later stages either a very low wind velocity or an optically thin circumstellar disk could produce the centred forbidden lines seen in the category IV stars presented here.

Finally we mention the suggestion (see Königl 1996) that the absence of a HVC in the [OI] emission of many HAEBESs may not be an evolutionary effect. Instead it is proposed that the absence of an [OI] HVC is caused by the lack of neutral oxygen, due to the photoionization near the outflow axis of the star. Königl (1996) proposes that in contrast the disk wind, responsible for the LVC emission, may not have this problem as it may be shielded, at least close to the disk, from the central radiation field. Although a plausible explanation, at least for the most luminous sources like MWC 297, if it were to be the case in general then one would expect most of our category II sources to be associated with extended outflows (seen, for example, in CO) and this is not the case. That is to say, there genuinely appears to be a lack of a HVC in many of these stars.

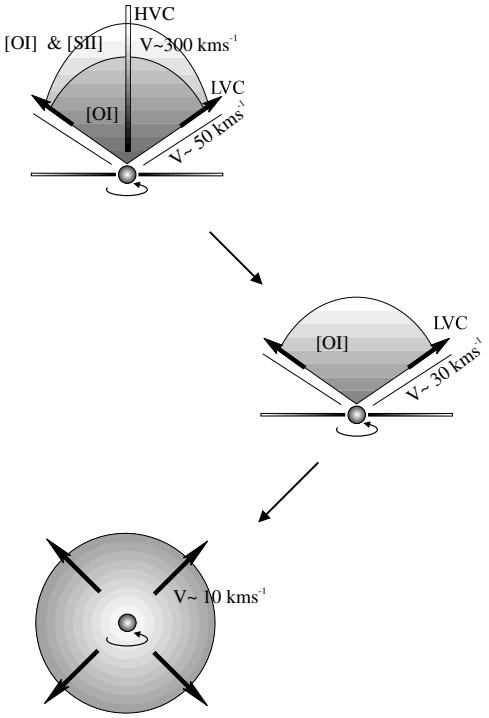

Fig. 3. Three evolutionary phases of the outflow envisaged from the observations. Firstly, top left, the category I stars associated with jets and molecular outflows have a powerful jet responsible of the HVC emission, with characteristic velocities of $\sim$ 300 kms^{-1}. A rotating disk wind or disk corona gives rise to the LVC emission with typical outflow velocities of 50 kms^{-1}and line broadening due to the rotation. As the system evolves the high velocity outflow dies off, leaving only the low velocity wind responsible for the LVC emission. The average radial LVC velocity of category IIa and IIb stars is lower than that of the category I stars. Eventually the circumstellar disk may become optically thin at radii where forbidden emission lines form. Narrow and centred forbidden emission lines result.

4.2. The nature and origin of the HVC and LVC

It is generally accepted that the observation of double-peaked forbidden line profiles in many cTTSs and certain HAEBESs provide evidence of two distinct velocity gas flows from such stars. The high velocity component is most readily explained as a jet forming deep in the gravitational well of the star, either at the stellar surface or within a few stellar radii and emerging from the system along the star's rotational axis. Certainly associating the HVC emission with the presence of a stellar jet appears warranted. In many observations where both components (HVC & LVC) are observed the radial velocities of the HVC match those observed for associated stellar jets and HH objects (e.g. HL Tau, Mundt et al. 1990; Z CMa, Poetzel et al. 1989; DG Tau, Mundt et al. 1987 and Solf & Böhm 1993). Where the HVC is extended (CW Tau, DO Tau, Hirth et al. 1994b; PV Cep, LkHα 233, Corcoran & Ray 1997b) there is clear evidence for the association of the HVC with the larger scale optical jet. A number of competing models have been proposed to explain the formation of high velocity jets and these have been addressed comprehensively in reviews by Königl & Ruden (1993) and Ray & Mundt (1993). In synopsis current theories favour either a stellar wind or disk wind as the source of the jet material and collimation via a magnetic field, either stellar or disk-generated

in origin. Optical jets are observed to be well collimated on scales smaller than 150–200 AU (Ray et al. 1996). Fendt et al. (1995) have examined the relativistic force-free equilibrium equation for the collimation of YSO winds by a relativistically rotating magnetosphere, originating in the star and reproduce the observed jet diameters well.

While the various models proposed have had success in modeling the jet component's emission, all the models that assume a single velocity law and single outflow from the young star naturally have difficulty in modeling the LVC emission. The LVC, however, is not readily explainable in term of a simple jet model. The low outflow velocities ($\leq$ 10 kms^{-1} in cTTSs, $\leq$ 80 kms^{-1} in HAEBESs) contrast with the broad width of the lines. Line widths of $\sim$ 100 kms^{-1} for the LVCs of cTTSs and $\sim$ 150–200 kms^{-1} for the LVCs of HAEBESs make a simple poorly collimated wind unlikely as edge-on viewing angles are *always* necessary to explain the large line widths but small centroid velocities. The simplest assumption to explain the broad line widths is that of rotational broadening. This in turn suggests a disk origin for the LVC, at least in the case of the cTTSs, as these low mass stars do not rotate at such high velocities. The arguments supporting such an origin are threefold. Firstly there is the combination of the low outflow velocity and the broad line widths as already mentioned. Secondly the observed luminosity of the forbidden lines, for example [SII]λ6716/6731, indicate an emitting region of several tens of AU in diameter (Edwards et al. 1987). Thirdly Hirth et al. (1994a) & Hartigan et al. (1995) have shown that there is a progression in the blueshifted velocities of LVC forbidden lines of young stars showing HVC+LVC emission. The species with the highest critical densities (e.g. [OI]λ5577) show the smallest blueshifted velocities, those with intermediate critical densities (such as [OI]λ6300) show higher blueshifted velocities and the species with the lowest critical density (e.g. [SII]$\lambda\lambda$6716/6731) show the highest blueshifted velocities. Similar behaviour is observed for all the stars listed in Table 2 except Z CMa and KK Oph (compare the [OI]λ6300 radial velocities in Table 1 and radial velocities of the [SII] lines in Table 2). The progression of increasing velocity with decreasing density is consistent with an accelerating wind from a disk (Solf & Böhm 1993; Böhm & Solf 1994; Hirth et al. 1994a; Hartigan et al. 1995). Kwan & Tademaru (1995) have recently extended their qualitative model to a simulation of a rotating disk wind to explain the origin of the LVC emission in cTTSs. The disk wind is driven by a magnetic torque and centrifugal flinging. Essentially the LVC is driven in a manner similar to the jet but, due to the lower initial z-velocity of the wind and its location further from the star, the overall acceleration is much less than that experienced by the HVC.

Having adopted an hypothesis of a disk wind as the origin of the LVC emission we can directly relate the width of the LVC line to the inner radius of the disk at which forbidden line emission is observed. Assuming the disk is in Keplerian rotation around the star then $V_{Kepler} \approx 26(10^{13} cm/r)^{1/2}(M_*/0.5M_\odot)^{1/2}$ kms^{-1} (Kwan & Tademaru 1995) gives the Keplerian velocity at radius r, assuming an eccentricity of 0. Taking the case of LkHα 233, where the line width of the LVC is about 150 kms^{-1}, the inner radius of the emission would be $\sim$ 0.1 AU or about 30 stellar radii (M_* = 2.6 $M_\odot$ and R_* = 2.6 $R_\odot$, Hillenbrand et al. 1992). Assuming a velocity of 10 kms^{-1} for the slowest material the outer edge of the forbidden line emission is at about 24 AU.

5. Conclusions

From our observations of 28 HAEBESs with detected [OI]λ6300 emission, a number of conclusions can be drawn:

- Herbig Ae/Be star forbidden [OI]λ6300 emission falls into one of four categories: I – strongly blueshifted emission, accompanied by a second emission component at a considerably lower, but still blueshifted, velocity, II – low velocity blueshifted emission similar to the low velocity component in category I, III – low velocity redshifted emission and IV – symmetric and unshifted emission.
- More than half the sample possess clearly blueshifted emission lines with radial velocities, $|v_c| \geq$ 10 kms^{-1}. There is no corresponding group of stars with even moderately redshifted forbidden emission and most of the remaining stars have unshifted lines within observational errors. Thus there is a close analogy with cTTSs where a similar asymmetry is taken as evidence for the presence of opaque circumstellar disks.
- The HVC forbidden line emission from HAEBESs is best interpreted in terms of a high velocity outflow, in keeping with the model of Kwan & Tademaru (1988, 1995). This is exemplified by the fact that all stars we observe with HVC emission are known jet sources. The LVC emission can be interpreted in terms of a disk wind, with a low velocity and rotationally broadened. Both the velocity and the width of the LVC appear to be larger than the corresponding component in cTTSs.
- The relatively small number (4/28) of HAEBESs with high velocity blueshifted forbidden line emission (category I) indicates a small number of HH jets in this class of young star, if the model of Kwan & Tademaru (1988) is correct and the HVC is evidence of a stellar jet. Direct imaging of HAEBESs (Corcoran & Ray 1997b) confirms this conclusion.
- It is possible to construct an evolutionary sequence based on the degree of outflow and forbidden emission line activity. Our category I stars, which are also Hillenbrand Group II stars (Hillenbrand et al. 1992), are all jet sources and are highly embedded. Such stars appear less evolved that our category II stars, which show lower blueshifted velocities and a reduced frequency of outflow activity, judged by the lower number of jets associated with the category. The lower velocities of the [OI]λ6300 emission in the category II stars may be due to the evolution of the outflow mechanism. The category III stars show low velocity redshifted emission and no association with jet or molecular outflow activity. The category IV stars show symmetric and unshifted (relative to the systemic velocity) [OI]λ6300 emission and are not generally believed to power outflow phenomena. Two category

IV stars, LkHα 234 and BD+46 3471, have been associated with an optical jet (LkHα 234, Ray et al. 1990) and a HH object (BD+46° 3471, Goodrich 1992) but there is some doubt, at least in the case of LkHα 234 (Weintraub et al. 1994), as to the true source of the outflow. Category IV stars may be regarded as more evolved than the category I and II stars.

– The presence of [SII] emission is predominantly detected in those stars with jets.

Acknowledgements. We would like to thank the referee, G. Gahm, for his helpful comments. MC would like to acknowledge funding from Fobairt, the Irish Science and Technology Agency. Thanks are also due to David Corcoran and Alan Moorhouse for their observations on the INT and ESO/MPI 2.2m Telescope respectively. Finally, we would like to express our gratitude to the staff of the La Palma Observatory for their help. The Isaac Newton Telescope on the island of La Palma is operated by the Royal Greenwich Observatory at the Spanish Observatorio del Roque de los Muchachos of the Instituto de Astrofisica de Canarias.

References

Allen, C.W., 1973, Astrophysical Quantities, The Athlone Press, University of London
Appenzeller, I. Jankovics, I., Krautter, J., 1983, A&AS 53, 291
Appenzeller, I., Jankovics, I., Östreicher, R., 1984, A&A 141, 108
Barth, W., Weigelt, G., Zinnecker, H., 1994, A&A 291, 500
Bastien, P., Ménard, F., 1990, ApJ 364, 232
Berrilli, F., Corciulo, G., Ingrosso, G., Lorenzetti, D., Nisini, B., & Strafella, F., 1992, ApJ 398, 254
Böhm, T., Catala, C. 1994, A&A 290, 167
Böhm, K. -H., Solf, J., 1994, ApJ 430, 277
Brugel, E.W., Mundt, R., Bührke, T., 1984, ApJ 287, L73
Cantó, J., Rodríguez, L.F., Barral, J.F., Carral, P. 1981, ApJ 244, 102
Cantó, J., Rodríguez, L.F., Calvet, N., Leverault R.M., 1984, ApJ 282, 631
Corcoran, D., Ray, T. P., Bastien, P. 1995, A&A 293, 550
Corcoran, M., Ray, T. P., 1997a, in press
Corcoran, M., Ray, T. P., 1997b, A&A in preparation
Edwards, S.E., Cabrit, S., Strom, S.E., Heyer, I., Strom, K.M., Anderson, E., 1987, ApJ 321, 473
Edwards, S.E., Ray, T.P., Mundt, R., 1993, in: Protostars and Planets III, Levy, E.H., Lunine, J.I., eds., (Tucson: University of Arizona), p. 567
Edwards, S.E., Snell, R.L., 1983, ApJ 270, 605
Evans, N.J., Balkum, S., Levreault, R.M., Hartmann, L., Kenyon, S., 1994, ApJ 424, 793
Fendt, C., Camenzind, M., Appl, S., 1995, A&A 300, 791
Finkenzeller, U., 1985 A&A 151, 340
Finkenzeller, U., Jankovics, I. 1984, A&AS 57, 285
Finkenzeller, U., Mundt, R., 1984 A&AS 55, 109
Fukui, Y., Iwata, T., Mizuno, A., Bally, J., Lane, A.P., 1993, in: Protostars and Planets III, Levy, E.H., Lunine, J.I., eds., (Tucson: University of Arizona), p. 603
Ghandour, L., Strom, S., Edwards, S., & Hillenbrand, L., 1994, in: The Nature and Evolutionary Status of Herbig Ae/Be Stars, eds. Thé, P.S., Pérez, M.R., & van den Heuvel, P.J., (Astronomical Society of the Pacific Conference Series Vo p. 223
Gledhill, T.M, Warren-Smith, R.F., Scarrott, S.M., 1987, MNRAS 229, 643
Goodrich, R.W., 1986, ApJ 311, 882
Goodrich, R.W., 1992, ApJS 86, 499
Grady, C.A., Pérez, M.R., Grinin, V.P., de Winter, D., Johnson, S.B., Talavera, A., 1995, A&A 302, 472
Graham, J., PASP 104, 479
Grinin, V.P., Kozlova, O.V., Thé, P.S., Rostopchina, A.N., 1996, A&A 292, 165
Grinin, V.P., Thé, P.S., de Winter, D., Giampapa, M., Rostopchina, A.N., Tambovtseva, L.V., Van Den Ancker, M.E., 1994, A&A 292, 165
Hamann, F., 1994, ApJS 93, 485
Hamann, F., Persson, S.E. 1989, ApJ 339, 1078
Hartigan, P., Edwards, S.E., Ghandour, L., 1995 ApJ 452, 736
Hartmann, L., Kenyon, S.J., Calvet, N., 1993, ApJ 408, 219
Hillenbrand, L.A., Strom, S.E., Vrba, F.J., Keene, J. 1992, ApJ 397, 613
Hirth, G.A., 1994, Ph.D. Thesis, University of Heidelberg
Hirth, G.A., Mundt, R., Solf, J., 1994a, A&A 285, 929
Hirth, G.A., Mundt, R., Solf, J., Ray, T.P., 1994b, ApJ 427, L99
Hollenbach, D., 1985, Icarus 61, 36
Königl, A., 1989, ApJ 342, 208
Königl, A., 1991, ApJ 370, L39
Königl, A., 1996, in: Proceedings of Disks and Outflows Around Young Stars, eds. Beckwith, S.V.W., Natta, A., & Staude, J., (Heidelberg: Springer Verlag), p.282
Königl, A., Ruden, S.P., 1993, in: Protostars and Planets III, Levy, E.H., Lunine, J.I., eds., (Tucson: University of Arizona), p. 641
Koresko, C.D., Beckwith, S., Ghez, A. M., Matthews, K., Herbst, T.M., Smith, D.A., 1993, AJ 105, 1481
Kwan, J., Tademaru, E. 1988, ApJ 322, L41
Kwan, J., Tademaru, E. 1995 ApJ 454, 382
Lada, C.J., Adams, F.C., 1992, ApJ 393, 278
Lang, K.R., 1991, Astrophysical Data: Planets and Stars (Springer-Verlag), p. 125.
Leinert, Ch, Haas, M., Lenzen, R., 1991, A&A 246, 180
Leverault, R.M., 1988, ApJS 67, 283
Malbet, F., Rigaut, F., Bertout, C., Lena, P., 1993, A&A 271, L9
Mendoza, E.E., 1983, in: "Planetary Nebulae", IAU symposium 103, D.R. Flower ed., (Dordrecht: Reidel), p. 143
Mundt, R., Brugel, E.W., Bührke, T., 1987, ApJ 319, 275
Mundt, R., Ray., T.P., 1994, in: "The Nature and Evolutionary Status of Herbig Ae/Be Stars", Thé, P.S., Pérez, M.R., van den Heuvel, E.P.J., eds., Astronomical Society of the Pacific Conference Series 62, 237
Mundt, R., Ray, T.P., Bührke, T., Raga, A.C., Solf, J., 1990, A&A 232, 37
Nakano, M., Tatematsu, K., 1990, PASJ 42, 567
Natta, A., Palla, F., Butner, H.M., Evans II, N.J., Harvey, P.M., 1993a, ApJ 406, 674
Natta, A., Prusti, T., Krugel, E., 1993b A&A 275, 527
Neckel, T., Staude, H.J., Sarcarder, M., Birkle, K., 1987, A&A 175, 231
Nisini, B., Milillo, A., Saraceno, P., Vitali, F., 1995, A&A 302, 169
Osterbrock, D.E., 1989, Astrophysics of Gaseous Nebulae and Active Galactic Nuclei, (Mill Valley California: University Science Books).
Padman, R., Richer, J.S., 1994, Ap&SS 216, 129
Piirola, V., Scaltriti, F., Coyne, G.V., 1992, Nat 359, 399
Poetzel, R., Mundt, R., Ray, T.P., 1989, A&A 224, L13
Poetzel, R., Mundt, R., Ray, T.P., 1992, A&A 262, 229
Ray, T.P., Poeztel, R., Solf, J., Mundt, R., 1990, ApJ 357, L45

Ray, T.P., Mundt, R., 1993, in: "Astrophysical Jets", STScI Symposium, Fall, M., O'Dea, C., Livio, M., Burgarella, D., eds. (Cambridge University Press) p. 145
Ray, T.P., Mundt, R., Dyson, J., Falle, S.A.E.G., Raga, A.C., 1996, ApJ 468L103
Reipurth, B., 1989, in: ESO workshop on Low Mass Star Formation and Pre-Main Sequence Objects, B. Reipurth, ed., (Garching: European Southern Obs.) p. 247
Rydgren, A.E., Schmelz, J.T., Vrba, F.J., 1982, ApJ 256, 168
Safier, P.N, 1993a, ApJ 408, 115
Safier, P.N, 1993b, ApJ 408, 148
Schulz, A., Black., J.H., Lada., C.J., Ulich, B.L., Martin, R.N., Snell, R.L., Erickson, N.J., 1989, ApJ 341, 288
Solf, J., Böhm, K.-H., 1993, ApJ 410, L31
Sorelli, C., Grinin, V.P., Natta, A., 1996, A&A 309, 155
Staude, H.J., Elsässer, H. 1993 ARA&A 5, 165
Strom, S.E., Edwards, S., Skrutskie, M.F., 1993, in: Protostars and Planets III, Levy E.H., Lunine J.I. eds., (Tucson: University of Arizona), p. 837
Thé, P.S., de Winter, D., Pérez, M.R. 1993, A&AS 104, 315
Verdes-Montenegro, L., Gómez, J.F., Torelles, J.M., Anglada, G., Estalella, R., López, R., 1991, A&A 244, 84
Weintraub, D.A., Kastner, J.H., Mahesh, A., 1994, ApJ 420, 87
Wolk, S.J., Walter, F.M., 1996, AJ, preprint
Yoshida, S., Kogure, T., Nakano, M., Tatematsu, K., Wiramihardja, S.D., 1991 PASJ 43, 363

This article was processed by the author using Springer-Verlag LaTeX A&A style file *L-AA* version 3.